Available online at www.sciencedirect.com
ScienceDirect
C. R. Mecanique 335 (2007) 638–654
COMPTES RENDUS MECANIQUE
http://france.elsevier.com/direct/CRAS2B/

Boussinesq approximation, convection

The Rayleigh–Benard problem in extremely confined geometries with and without the Soret effect

Jean K. Platten [a,*], Manuel Marcoux [b], Abdelkader Mojtabi [b]

[a] *University of Mons-Hainaut; B-7000 Mons, Belgium*
[b] *IMFT, Allée du Professeur Camille-Soula, 31400 Toulouse, France*

Received 24 October 2006; accepted after revision 11 April 2007

Available online 27 September 2007

Abstract

We examine the linear stability of a liquid layer heated from below (the classical Rayleigh–Benard problem) but laterally confined between four vertical rigid and adiabatic boundaries. The main feature of the present study is that the height of the layer is much greater than the two other horizontal dimensions. The Soret effect is also taken into account. The ultimate objective of the study is a better knowledge of the operation of thermogravitational columns, and the search for a possible new way to measure positive Soret coefficients based on the variation of the critical Rayleigh number. ***To cite this article: J.K. Platten et al., C. R. Mecanique 335 (2007).***

Résumé

Le problème de Rayleigh–Bénard dans des géométries extrêmement confinées avec et sans effet Soret. On examine la stabilité linéaire d'une couche liquide chauffée par le bas (le problème classique de Rayleigh–Bénard) mais confinée latéralement par quatre parois rigides et adiabatiques. La caractéristique essentielle de cette étude est que la hauteur de la couche est beaucoup plus grande que les deux autres dimensions horizontales. On prend aussi en compte l'effet Soret. L'objectif ultime de cette étude est une meilleure connaissance du mode opératoire de colonnes thermogravitationnelles ainsi que la recherche d' une méthode nouvelle pour mesurer des coefficients Soret positifs, basée sur la variation du nombre de Rayleigh critique. ***Pour citer cet article : J.K. Platten et al., C. R. Mecanique 335 (2007).***

Keywords: Computational fluid mechanics; Rayleigh–Benard; Stability; Galerkin; Thermodiffusion; Soret

Mots-clés : Mécanique des fluides numérique ; Rayleigh–Bénard ; Stabilité ; Galerkin ; Thermodiffusion ; Soret

1. Introduction

The onset of free convection in horizontal liquid layers heated from below and of infinite extent in the two horizontal directions (the so-called Rayleigh–Benard problem) is well known both for a pure liquid and for a binary mixture

* Corresponding author.
E-mail address: Jean.platten@skynet.be (J.K. Platten).

1631-0721/$ – see front matter
doi:10.1016/j.crme.2007.08.011

taking into account the Soret effect [1,2]. Its extension to the case of through flow of Poiseuille type has also been considered [3–6]. In all these studies the critical Rayleigh number, eventually its variation with the separation ratio (the ratio of the solutal to the thermal contribution to the buoyancy) or with the Reynolds number, were given together with the critical wave number.

Much less is known when the fluid layer is laterally bounded by rigid boundaries. In that case two aspect ratios, say 'height to length' and 'height to depth', influence the critical Rayleigh number and the convective pattern as well. The study is usually restricted to small aspect ratios generally not exceeding 1. For example in a rectangular cavity, the rolls are aligned (at least with no through flow) with their axes parallel to the shorter side of the container [7]. In this article we deal with aspect ratios much greater than 1 and the system we investigate is shown on Fig. 1. The two aspect ratios H/L and H/P are both much greater than 1 and sometimes of the order of 10^2. The two shadowed horizontal boundaries at $z = 0$ and $z = H$ are at constant temperature T_1 and T_2 with $T_1 > T_2$, while the four lateral boundaries will be adiabatic.

We now justify the reasons of this study. There are essentially two reasons both related to the Soret effect. The first reason is to understand how thermogravitational columns do operate. In thermogravitational columns, the geometry is fundamentally the same as that sketched on Fig. 1. However, the thermal conditions are totally different than in the Rayleigh–Benard configuration. In thermogravitational columns, the left and right boundaries at $x = 0$ and $x = L$ are kept at two different temperatures T_1 and T_2 and the cell is filled with a binary fluid. Bottom and top boundaries are e.g. adiabatic. Due to the Soret effect induced by the horizontal temperature gradient $\partial T/\partial x$, one of the components will migrate to the cold wall while the other component will migrate to the hot wall. The horizontal temperature gradient induces not only molecular separation, but also convection with hot fluid raising and cold fluid sinking. As a consequence of this basic convection (there is no threshold for the onset of this type of convection) the component that migrates to the hot wall is advected to the top and the component that migrates to the cold wall is advected to the bottom. Thus the interplay between convection and Soret effect destroys in some sense, at least partially, the horizontal concentration or mass fraction gradient but builds up vertical concentration stratification. Two cases must be considered. If the denser component goes to the cold wall and the lighter component to the hot one, then the resulting vertical concentration gradient will be stabilizing with dense fluid at the bottom and light fluid at the top. Almost the totality of the experiments was done in such a situation. We have to mention here that in many cases experiments are performed not in parallelepipedic cavities, but between two concentric cylinders kept at two different temperatures (see Fig. 2) (see e.g. [8–10]). As far as the spacing between the two cylinders $R_o - R_i$ (where R_o and R_i are the radii of the outer and inner cylinder respectively) remains small compared to the mean radius $R_M = (R_o + R_i)/2$ (no significant curvature effect), then there is some analogy between the two geometrical configurations, provided that $L = R_o - R_i$ and $P = 2\pi R_M$. Experiments have proved that the same Soret coefficient is obtained [11,12] independently of the type of cell used, parallelepipedic or cylindrical. However, the situation is totally different when the denser component migrates to the hot wall and the lighter component to the cold wall, in which case convection builds up an adverse vertical concentration gradient with dense fluid at the top of the cell and light fluid at the bottom. Parallelepipedic thermogravitational columns are unable to sustain this potentially unstable stratification, except maybe for small time, whatever the applied temperature difference between the two lateral walls [13,14]. On the contrary, between concentric cylinders it has experimentally been shown that this unstable stratification may be maintained in the steady state provided that the Grashof number (or the nondimensional temperature difference between the two cylinders) exceeds some critical value [15]. This is experimental observation only, not sustained by theoretical considerations. It seems to us that these apparent contradictory behaviours between the two types of columns must be related to some instability problems. Let us be a little more specific and recall the value of the molecular separation ΔC between the top and the bottom of a thermogravitational column given a long time ago by the Furry–Jones–Onsager–Majumdar theory [16,17]:

$$\Delta C = 504 \frac{\nu}{\alpha g} D_T C_0 (1 - C_0) \frac{H}{L^4} \tag{1}$$

In this last equation, ν is the kinematic viscosity of the fluid, α its thermal expansion coefficient, g the acceleration due to gravity, C_0 the initial, or mean mass fraction of the considered component, D_T its thermodiffusion coefficient in the mixture, H and L (or equivalently $R_o - R_i$) respectively the height and the spacing of the column according to Figs. 1 and 2. Let us note that P (or the mean radius) does not affect the molecular separation. One could also be astonished that the separation is independent of the applied temperature difference: in fact Eq. (1) is an approximation valid for

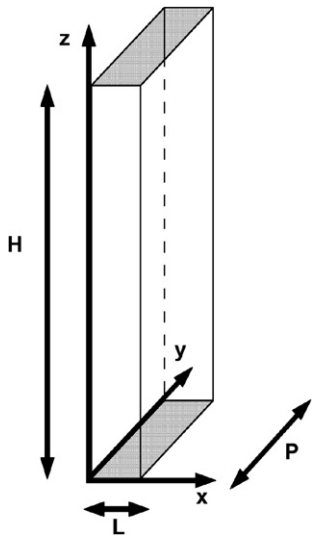

Fig. 1. Sketch of the system.
Fig. 1. Croquis du système.

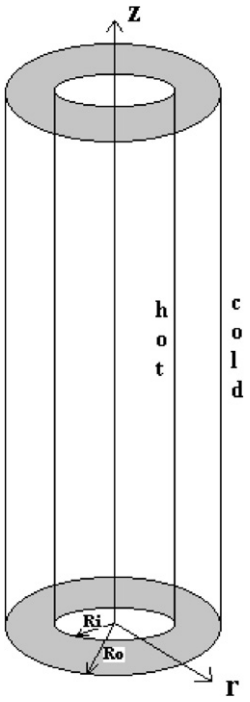

Fig. 2. A cylindrical thermogravitational column.
Fig. 2. Colonne thermogravitationnelle cylindrique.

'large gaps' (say greater than 1 mm); for gaps of the order 100–300 μm, the separation is an increasing function of the applied temperature difference, but we shall not deal in the remainder of this paper with such small gaps. Furthermore, the separation given by Eq. (1) has been obtained under the consideration of a constant thermodiffusion coefficient D_T. This remains a quite reasonable assumption when the separation is small ($\Delta C/C_0 \sim 0.01$–0.1), namely for 'large gap' thermogravitational columns, but could be less satisfactory for larger separations since it is well known that D_T is concentration dependent. This extension of the separation, considering a temperature and concentration dependent Soret coefficient (the ratio of D_T divided by the isothermal molecular diffusivity D) is given in this volume in a paper by Labrosse [18].

Next, we define as usual a Rayleigh number (in the present case a solutal Rayleigh number) by

$$Ra_S = \frac{g\beta \Delta C H^3}{\nu D} \tag{2}$$

where β is the mass expansion coefficient and D the isothermal (or molecular) diffusion coefficient. By combining Eqs. (1) and (2) we get

$$Ra_S = 504 \frac{\beta}{\alpha} \frac{D_T}{D} C_0(1 - C_0) \left(\frac{H}{L}\right)^4 \tag{3}$$

In most problems coupling Soret effect and convection one usually defines a so-called separation ratio S by

$$S = \frac{\beta}{\alpha} \frac{D_T}{D} C_0(1 - C_0) \tag{4}$$

This separation ratio represents the solutal contribution to the buoyancy divided by the thermal contribution. Combining Eqs. (3) and (4) we get

$$Ra_S = 504 S \left(\frac{H}{L}\right)^4 \tag{5}$$

Summarizing, the interplay between Soret effect and free convection builds up a vertical density gradient measured by the solutal Rayleigh number (5) containing the thermodiffusive properties of the mixture (S) and one of the as-

pect ratios (H/L). This density gradient (sometimes adverse depending on the sign of S) is solely due to the vertical concentration gradient since the temperature is not a function of the vertical coordinate z. The stability of this steady state solution is not easy because of the existence of a basic velocity profile; the vertical velocity is a function of x (or r), temperature is also a function of x (or r), but concentration is a function of x and z. Of course one could try to handle the complete problem, but in a first step we could simplify it. This simplification is based on experimental considerations. The gap between the two walls (or the two cylinders) is of the order of 1 mm (at most 2 mm), otherwise according to Eq. (1) greater spacings would produce molecular separation too small to be detected. Also in the experiments the height H is of the order of 500 mm in order to observe a sufficient and measurable molecular separation. And even in such geometrical conditions the molecular separation will be of a few percent only; higher separations (say 30% or even more) can be obtained with smaller gaps, typically ∼200–300 μm [16,19], but this raises many other technical problems. Thus with an aspect ratio H/L of the order of say 300, the effective solutal Rayleigh number at which we operate is according to Eq. (5) of the order of $Ra_S \sim 4 \times 10^{12} S$. Even for a small separation ratio of the order of $S \sim 0.1$, we are operating at very high solutal Rayleigh numbers, which could be supercritical. However, as we said before, let us simplify the stability problem. Suppose that when the steady state is reached we turn off the temperature gradient (say the two thermostats). Immediately, or almost immediately because of the small gap and the high thermal diffusivity of the liquid mixture in comparison with its molecular diffusivity, the temperature will become uniform; as a consequence the flow stops. But the vertical concentration gradient will take months or years to disappear by diffusion because of the smallness of the molecular diffusivity and the large value of H. Therefore we are left with a cavity into which there is only an adverse vertical density gradient, its origin being solutal, due to the interplay 'in the past' between Soret effect and convection (which has been stopped for a while); in other words we have to face with an ordinary Rayleigh–Benard problem, except that we are working in extremely confined geometries (which is not so usual) and for aspect ratios corresponding to experiments with thermogravitational columns we did not find in the literature any useful information. Thus the motivation is first to know how the critical Rayleigh number equal to 1707.762 in infinite horizontal layers will be affected by an extreme lateral confinement; next what are the most dangerous perturbations and last if the solutal Rayleigh number at which thermogravitational columns do operate and given by Eq. (5) is smaller or higher than the critical Rayleigh number. The answer to these questions could not be the same in Cartesian co-ordinates (parallelepipedic cavity) and in cylindrical co-ordinates (a liquid layer between two concentric cylinders); and in the last case it is not sure that axisymmetric perturbations are the most dangerous as far as the stability of the system is concerned; azimuthal modes have to be considered.

This is our first motivation for investigating the Rayleigh–Benard problem in extremely confined geometries. But there is a second motivation.

In the classical Rayleigh–Benard problem of binary liquid layers of infinite horizontal extension heated from below, the critical Raleigh number will be modified by the Soret effect [2,20]. This modification is directly related to the separation ratio S. Therefore if we are able to measure with the requested accuracy the modification of the critical Rayleigh number and if we have correct working equations that give the variation of the critical Rayleigh number with the separation ratio S, then this will be an indirect way, but nevertheless accurate way, to determine a separation ratio and from its numerical value a Soret coefficient without any sampling process followed by a compositional analysis of the removed samples [21–23]. The price we have to pay is a precise knowledge of the two expansion coefficients, but this is not a problem since commercial densimeters are available with an accuracy of 2×10^{-6} g/cm^3 (quartz U-tube vibrating densimeter). Once again two cases must be considered depending on the sign of the separation ratio.

When $S < 0$, the solutal contribution is of opposite sign to that of the thermal contribution; since the thermal contribution is destabilizing (we heat from below), the solutal contribution is stabilizing. In other words the denser component migrates to the bottom plate (to the hot) and the adverse density gradient (due to the temperature gradient) is reduced by the Soret effect. As a consequence we need a larger temperature difference (or thermal Rayleigh number) to promote convection. Thus the increase of the critical thermal Rayleigh number is a measure of S. It is rather easy to detect the onset of free convection. In the past Schmidt–Milverton plots were employed [24,25], but today we have at our disposal modern optical techniques as for example Laser-Doppler Velocimetry, provided that the equipment is dedicated to measure extremely small velocities, down to e.g. 5 μm/s. But this is actually the case [26]. To be more concrete, for a layer of water 4.15 mm height, the necessary temperature difference for the onset of convection is 1.7 °C [27]. The situation is therefore not too bad since the temperature of each boundary (say each copper plate) may be controlled at ±0.01 °C with commercial thermostats. The addition of a small amount of salt or a particular alcohol (ethanol or propanol) will increase considerably this critical temperature difference, say up

to 2.5 or 3 °C or more; the computed new critical thermal Rayleigh number, larger than 1707.762, finally gives the separation ratio S. Moreover in that case it is well known that the bifurcation is an Hopf bifurcation characterized by its Hopf frequency, also related to the separation ratio [20,21,25,28]. And since one is able to measure at a given point inside the system the velocity say each second, or each two seconds, from the time dependence of the velocity (well before saturation due to the nonlinear terms), having Fourier transformed the oscillatory time trace, we get the Hopf frequency and thus a second independent measurement of the separation ratio. This procedure is currently used since 15 years [22,23]. Very precise values may be obtained for the Soret coefficient that are in remarkable agreement [21] with other techniques like the bending of a laser beam [28,29], or more recently the very efficient Thermal Diffusion Forced Rayleigh Scattering technique, a very sophisticated optical technique based on the existing temperature gradients due to light adsorption inside a system of interference fringes created at the intersection of two laser beams [30]. Light is thus used to create the temperature gradient, more precisely a temperature grating. And Soret effect induces a concentration grating. The resulting index of refraction grating is read out by Bragg diffraction by a second laser.

When $S > 0$, the solutal contribution is of the same sign as that of the thermal contribution and therefore also destabilizing. In other words the denser component migrates to the cold upper plate and convection will start earlier: the critical Rayleigh number is reduced. One could think of using this fact as a measure of the separation ratio, as we did for negative separation ratios. However this will not work for accuracy reasons. To be more specific let us give the critical thermal Rayleigh number for the onset of *steady* convection (which is the case for $S > 0$ in contradistinction with the oscillatory onset for $S < 0$)

$$Ra^{\text{crit}} = \frac{27\pi^4}{4} \frac{1}{1 + S(Le + 1)} \tag{6a}$$

This last equation has been established for the case of stress-free, conducting and pervious boundaries, which could be nonrealistic as far as experiments are concerned but this is not the main point. For realistic boundary conditions (rigid, conducting and impervious) convection starts (at zero wavenumber) with a critical Rayleigh number given by [31]

$$Ra^{\text{crit}} = \frac{720}{Le\, S} \tag{6b}$$

Le is the Lewis number, the ratio of the thermal diffusivity κ by the molecular diffusivity D. It is well known in liquids that heat diffuses much more rapidly than mass, typically 100 to 1000 times faster. Thus $Le \sim 100$–1000. For example, salty water 0.5 M/l NaCl has a Lewis number of 140 [32] and a solution water (90 wt%)-isopropanol (10 wt%) has a Lewis number of 200 [22]. Thus according to Eqs. (6), the critical Rayleigh number will be reduced by at least a factor 20 in most realistic cases. In other words, if the critical temperature difference to observe the onset of free convection in absence of the Soret effect is of the order of 2 °C (a very convenient value for accurate experimental work), this temperature difference will drop to 0.1 °C under the influence of the Soret effect. One recognizes immediately the loss of accuracy in the determination of a positive S by the use of the critical point for the onset of free convection. Of course, one could always try to build thermostatisation systems constant at ± 0.001 °C or better, but this has not yet been done. Thus, the determination of positive separation ratios or Soret coefficients was never made in a Rayleigh–Benard configuration. Imagine now critical Rayleigh numbers for pure fluids ($S = 0$) much higher than $27\pi^4/4$ or 1708, for example 10^6 or 10^9, simply due to a lateral confinement of the layer that will delay the onset of convection. In order to get such high values of the critical Rayleigh number, one needs cavities of the type sketched on Fig. 1. Suppose now that a Rayleigh number as high as 10^6 or 10^9 (it does not matter) implies a totally unrealistic temperature difference of 100 °C. After reduction by a factor of 20 due to the Soret effect, this temperature difference will drop to the very convenient value for an experimentalist of 5 °C. Thus one of the objectives is to search a new possible way to measure positive separation ratios by convective coupling. But first we have to conceive an experimental cell, i.e. we have to determine the two aspect ratios that will provide optimal conditions for experiments. Thus we have to solve the Rayleigh–Benard problem in the geometry of Fig. 1 and to find the variation (at $S = 0$) of the critical thermal Rayleigh number with the two aspect ratios H/L and H/P. Next we have to extend the problem with the Soret effect included, since it would be hazardous to suppose the validity of Eq. (6a) in the form

$$Ra^{\text{crit}} = Ra_0^{\text{crit}}\left(\frac{H}{L}, \frac{H}{P}\right) \frac{1}{1 + S(Le + 1)} \tag{7}$$

where Ra_0^{crit} is the aspect ratios dependent critical value of the Rayleigh number at $S = 0$. In fact we can prove that Eq. (7) is not true.

Thus there several reasons to undertake the linear stability of liquid layers with an adverse density gradient in extremely confined geometries with and without the Soret effect.

2. The Rayleigh–Benard problem in confined cavities for pure fluids

In this article, the Boussinesq approximation [33] is used. It states that density differences $\delta\rho$ between two points in the fluid are sufficiently small to be neglected, except where they appear in terms multiplied by g, the acceleration due to gravity. The Boussinesq approximation is inaccurate when the nondimensionalised density difference $\delta\rho/\rho$ is of order unity. Since in many problems of natural convection we use an equation of state of the form $\rho = \rho_0(1 - \alpha\Delta T)$ where α is the thermal expansion coefficient, generally lower than 10^{-3} K^{-1}, and ΔT some applied temperature difference between boundaries, it is clear that the approximation will fail for temperature differences greater than 10^2 K. All this is discussed in details in [1]. Moreover we also make the approximation that the other physico-chemical parameters such as the viscosity, the thermal conductivity, the specific heat are temperature independent.

We consider the cavity represented on Fig. 1 with the lower wall at $z = 0$ at temperature T_1 (or concentration C_1) and the upper one at $z = H$ at T_2 (or C_2), with $T_1 > T_2$ (or $C_2 > C_1$ where C could represent some salt concentration). The four lateral boundaries will be adiabatic (or impervious to matter). There is complete analogy between the thermal and the solutal problems as long as they are acting alone. In fact, we investigate the stability of a basic rest steady state $V_i^{\text{steady}} = 0$ with a vertical temperature gradient $\partial T^{\text{steady}}/\partial z = \Delta T/H$ (or equivalently a vertical concentration gradient, or more precisely a vertical adverse density gradient, independently of its origin) and therefore in the remainder of this paper, V_i and T denote 'perturbations' around this basic state. We also suppose everywhere in the paper marginal stability. The real three-dimensional problem with three velocity components function of the three coordinates is rather difficult and therefore we only deal in this paper with rolls, i.e. two velocity components but still function of the three coordinates due to the lateral confinement. A roll has a symmetry axis that can be parallel to the x or to the y axis. Therefore two cases must be considered: x-rolls (Fig. 3) and y-rolls (Fig. 4) and we have to find out the most dangerous perturbations leading to the smallest Rayleigh number.

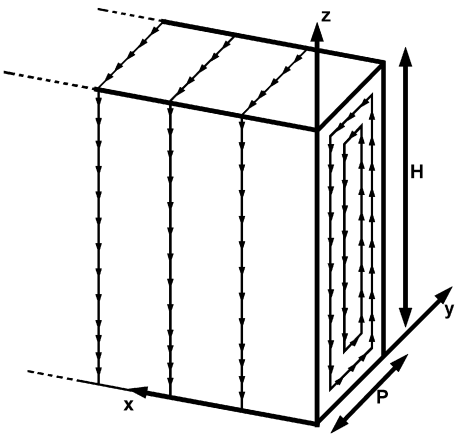

Fig. 3. (Infinite) x-rolls.

Fig. 3. Rouleau (infini) à l'axe x.

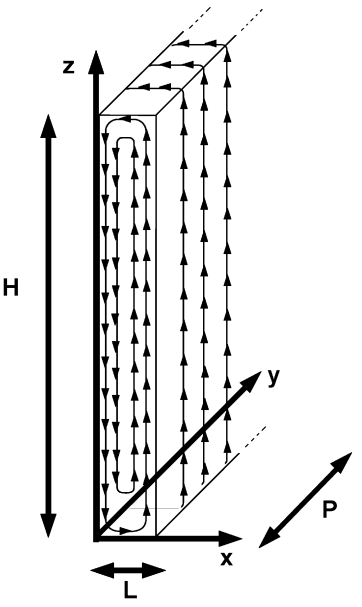

Fig. 4. y-rolls.

Fig. 4. Rouleau à l'axe y.

2.1. Simplified 1-D model

We first recall the 1-D problem, that is to say the flow problem in a plane (z–y or z–x, no matter) of very high aspect ratio ($H \gg L$ or P) such that the different fields are independent of the vertical coordinate z [34,35]. An analytical solution is available in this case. Thus we have only one vertical velocity component V_z function of one coordinate (say x). In such conditions, the steady linearized nondimensional Navier–Stokes and energy equations are in the Boussinesq approximation:

$$\frac{\partial^2 V_z}{\partial x^2} + Ra\,\Gamma^2 T = 0 \tag{8}$$

$$\Gamma^2 V_z + \frac{\partial^2 T}{\partial x^2} = 0 \tag{9}$$

where Ra is the Rayleigh number based on H^3 and Γ is the aspect ratio defined by $\frac{1}{\Gamma} = \frac{H}{L}$. (It could equally well be defined with P instead of L, replacing x by y into Eqs. (8), (9).) The boundary conditions associated to this problem are:

$$V_z = 0 \quad \text{at } x = 0 \text{ and } x = 1 \text{ (no slip)} \tag{10}$$

$$\frac{\partial T}{\partial x} = 0 \quad \text{at } x = 0 \text{ and } x = 1 \text{ (vertical walls are adiabatic)} \tag{11}$$

It is rather easy to eliminate T between Eqs. (8) and (9) and to solve

$$\frac{\partial^4 V_z}{\partial x^4} = \lambda^4 V_z \tag{12}$$

where $\lambda^4 = Ra\,\Gamma^4$ could be considered as a new Rayleigh number based on the distance L between the two lateral walls and on the vertical temperature gradient. The boundary conditions associated to (12) are

$$V_z = \frac{\partial^3 V_z}{\partial x^3} = 0 \quad \text{at } x = 0 \text{ and } x = 1 \tag{13}$$

The last boundary condition (13) is equivalent to (11) and deduced from Eq. (8). The general solution of Eq. (12) is

$$V_z = a\sin(\lambda x) + b\cos(\lambda x) + c\sinh(\lambda x) + d\cosh(\lambda x) \tag{14}$$

and for nontrivial solutions to exist satisfying the boundary conditions (13) we must have

$$1 - \cos\lambda\cosh\lambda = 0 \tag{15}$$

The smallest root of this equation is $\lambda = 4.73004074448627\ldots$ or in other words

$$Ra^{\text{crit}} = \frac{500.5639017\ldots}{\Gamma^4} \tag{16}$$

This result does apply to infinite x-rolls (Fig. 3) with $1/\Gamma = H/P$ or to infinite y-rolls (Fig. 4) with $1/\Gamma = H/L$ provided that there is no dependence of the different fields on the infinite direction (zero wavenumber in that direction). The confinement of the rolls (finite x- or y-rolls) will produce a higher critical Rayleigh number as we shall see later.

Let us apply this result (16) to real experiments in thermogravitational columns [11,13]. The dimensions of the cell used in these experiments are

$$H = 530 \text{ mm}, \qquad L = 1.58 \text{ mm}, \qquad P = 30 \text{ mm}$$

Therefore:

$$Ra^{\text{crit}}(\text{infinite } y\text{-rolls}) = 0.633781 \times 10^{13} \quad \text{and} \quad Ra^{\text{crit}}(\text{infinite } x\text{-rolls}) = 0.487621 \times 10^{8}$$

According to Eq. (5), the Rayleigh number at which the column operates is:

$$Ra_S = 0.638125 \times 10^{13} S$$

Since the order of magnitude of the separation ratio is $S \sim 0.01$ to 0.6, y-rolls are not dangerous but it seems that we are always operating above the critical Rayleigh number for *infinite* x-rolls. However the confinement will increase the

critical Rayleigh numbers and the question is to know if the working (solutal) Rayleigh number will remain above that corresponding to finite x-rolls. Thus we have to treat the case of *finite* x-rolls with two velocity components function of the three coordinates. In that case, an exact solution comparable to Eq. (16) does not exist, and approximate solutions (e.g. of Galerkin type) should be searched. This is the subject of the next paragraph.

2.2. Finite x-rolls

We are dealing here with the case $V_x = 0$; $V_z(x, y, z) \neq 0$; $V_y(x, y, z) \neq 0$. This can only be an approximation (probably excellent) since due to the boundary conditions such a flow cannot exist as shown e.g. in Chap. VI of [2]. But within the frame of this approximation we may define a stream function ψ by $V_z = -\frac{\partial \psi}{\partial y}$; $V_y = \frac{\partial \psi}{\partial z}$. For the nondimensional space coordinates, we use x/L, y/P and z/H. Once again as in Section 2.1, aspect ratios will appear in the nondimensional equations. They read:

$$\nabla^2\left(\frac{\partial^2\psi}{\partial z^2} + \frac{1}{B^2}\frac{\partial^2\psi}{\partial y^2}\right) = \frac{Ra}{B}\frac{\partial T}{\partial y} \tag{17}$$

$$\frac{1}{B}\frac{\partial \psi}{\partial y} = \nabla^2 T \tag{18}$$

with

$$\nabla^2 = \frac{\partial^2}{\partial z^2} + \frac{1}{A^2}\frac{\partial^2}{\partial x^2} + \frac{1}{B^2}\frac{\partial^2}{\partial y^2}; \qquad \frac{H}{L} = \frac{1}{A}; \qquad \frac{H}{P} = \frac{1}{B} \tag{19}$$

Before solving this 3-D problem, let us once again suppose that $H/L \gg 1$ and $H/P \gg 1$. In other words, the fields ψ and T do not depend on z: we only have one velocity component V_z function of y and also of x due to the lateral confinement in these two directions. Then Eqs. (17)–(19) reduce to

$$\nabla^2_{x,y} V_z = -Ra\, T \tag{20}$$

$$(-V_z) = \nabla^2_{x,y} T \tag{21}$$

$$\nabla^2_{x,y} = \frac{1}{A^2}\frac{\partial^2}{\partial x^2} + \frac{1}{B^2}\frac{\partial^2}{\partial y^2}; \qquad \frac{H}{L} = \frac{1}{A}; \qquad \frac{H}{P} = \frac{1}{B} \tag{22}$$

It is rather easy to eliminate T between Eqs. (20) and (21). We get:

$$\nabla^4_{x,y} V_z = Ra\, V_z; \qquad \nabla^4_{x,y} = \frac{1}{A^4}\frac{\partial^4}{\partial x^4} + \frac{2}{A^2B^2}\frac{\partial^2}{\partial x^2}\frac{\partial^2}{\partial y^2} + \frac{1}{B^4}\frac{\partial^4}{\partial y^4} \tag{23}$$

This generalises in some sense Eq. (12). Due to the cross-differentiation term in $\nabla^4_{x,y}$, a solution under the form $V_z(x, y) = F(x) + G(y)$ exists, but cannot satisfy the no slip boundary conditions, e.g.

$$V_z(0, y) = F(0) + G(y) = 0 \quad \forall y$$

Moreover, when solving Eq. (23), the additional boundary conditions on V_z reflecting a zero heat flux across the four lateral boundaries will make the problem even more complicated. Therefore we prefer to solve the system (20), (21) by a classical Galerkin technique. Let us now recall the boundary conditions associated to Eq. (20), (21):

$$\text{For } y = 0 \text{ or } 1,\ \forall x,\ V_z = 0 \text{ and } \partial T/\partial y = 0 \tag{24a}$$

$$\text{For } x = 0 \text{ or } 1,\ \forall y,\ V_z = 0 \text{ and } \partial T/\partial x = 0 \tag{24b}$$

Since we want to describe a finite x-roll, V_z must be antisymmetric with respect to $y = 1/2$, but is symmetric with respect to $x = 1/2$. The following sets of trial functions have all the required properties

$$V_z = \sum_{i=1}^{N}\sum_{j=1}^{N} a_{ij}\, y(y-1)(y-1/2)^{2i-1} x^j (1-x)^j \tag{25}$$

$$T = \sum_{i=1}^{N}\sum_{j=1}^{N} b_{ij}\left[(2y-1)^{2i-1} - \frac{2i-1}{2i+1}(2y-1)^{2i+1}\right]\left[(2x-1)^{2(j-1)} - \frac{j-1}{j}(2x-1)^{2j}\right] \tag{26}$$

Table 1
Convergence of $Ra.B^4$ in the 2-D problem as a function of the cross section aspect ratio B/A

Tableau 1
Convergence de $Ra.B^4$ dans le problème 2-D en fonction rapport d'aspect transversal B/A

N	$B/A = 1/100$	$B/A = 1/10$	$B/A = 1$	$B/A = 5$	$B/A = 10$	$B/A = 30/1.58$
1	627.214933	628.693333	776.533333	4360.533333	15560.533333	54464.726037
2	500.673104	507.158644	708.575710	4038.106322	13925.185435	47998.043147
3	500.630914	506.132529	707.993547	4020.583116	13666.503808	46463.928765
4	500.628147	505.721409	707.974387	4019.436741	13624.628794	45982.247429
5	500.626804	505.563706	707.972141	4019.273073	13619.217616	45844.024513
6	500.626006	505.512828	707.971704	4019.234419	13618.372794	45810.398023
7	500.625465	505.498772	707.971590	4019.223712	13618.139530	45803.111696
8	500.625060	505.495220	707.971552	4019.220229	13618.056534	45801.367095

But instead of solving Eq. (20), (22) for various values of A and B, we prefer to solve the problem for the cross section aspect ratio $(B/A) = (P/L)$ and find the numerical values of $Ra.B^4$ considered as eigenvalue of the problem. Indeed Eqs. (20), (21) may be rewritten as

$$\left(\frac{B}{A}\right)^2 \frac{\partial^2 V_z}{\partial x^2} + \frac{\partial^2 V_z}{\partial y^2} = -\left(Ra.B^4\right) T \tag{27}$$

$$\left(\frac{B}{A}\right)^2 \frac{\partial^2 T}{\partial x^2} + \frac{\partial^2 T}{\partial y^2} = -V_z \tag{28}$$

We give in Table 1 examples of convergence of $Ra.B^4$ for different values of B/A.

First of all the limit given by Eq. (16) is recovered for $B/A \to 0$ (infinite x-rolls). However, to be clear, only results for $B/A > 1$ have a physical meaning while the calculations with $B/A < 1$ is a mathematical game (when $B/A < 1$, the finite x-roll represented by the expansion (25) is aligned with its axis parallel to the larger side of the cell!). The confinement in the x-direction increases the critical Rayleigh number. The convergence is slower for extremely confined layers, as e.g. for the experimental case ($P = 30$ mm; $L = 1.58$ mm; last column), but remains not bad (0.3% difference between $N = 4$ and $N = 5$, which is far below any experimental error on a Rayleigh number; 0.07% difference between $N = 5$ and $N = 6$; and less than 0.02% between $N = 6$ and $N = 7$). Having the value of $Ra.B^4$, we may deduce Ra for any height of the column, but still subjected to the condition $H/L \gg 1$ and $H/P \gg 1$. For example for the experimental case evoked in Section 2.1 [11,13] ($H = 530$ mm; $L = 1.58$ mm; $P = 30$ mm) we get:

For	Finite x-rolls : $Ra = 45801.37 \times (530/30)^4 = 0.446166 \times 10^{10}$
To be compared to	Infinite x-rolls : $Ra = 0.487621 \times 10^8$
And to the	Operating Rayleigh number : $Ra = 0.638125 \times 10^{13} S$

Thus even if the x-confinement of the roll increases the critical Rayleigh number by two orders of magnitude, for usual values of S we are still operating above the instability point.

We have now to handle the full 3-D problem (Fig. 1) taking into account the confinement in the z direction (this will still increase the critical Rayleigh number) and described by the full Eqs. (17), (18). The boundary conditions are:

(1) zero velocity on the six faces and this implies

$$\begin{aligned} &\text{at } x = 0 \text{ and } 1 \quad \psi = 0 \\ &\text{at } y = 0 \text{ and } 1 \quad \psi = 0 \text{ and } \frac{\partial \psi}{\partial y} = 0 \\ &\text{at } z = 0 \text{ and } 1 \quad \psi = 0 \text{ and } \frac{\partial \psi}{\partial z} = 0 \end{aligned} \tag{29}$$

(2) temperature is prescribed on the bottom and top boundaries

$$\text{at } z = 0 \text{ and } 1 \quad T = 0 \tag{30}$$

(3) no heat flux across the four lateral boundaries

$$\begin{aligned} &\text{at } y = 0 \text{ and } 1 \quad \frac{\partial T}{\partial y} = 0 \\ &\text{at } x = 0 \text{ and } 1 \quad \frac{\partial T}{\partial x} = 0 \end{aligned} \tag{31}$$

Regarding the symmetry requirements,

V_z must be even in x, odd in y and even in z
V_y must be even in x, even in y and odd in z

and this implies:

ψ must be even in x, in y and in z

Finally:

T must be even in x, odd in y and even in z

The following expansions obey all the requirements

$$\psi = \sum_{i=1}^{N}\sum_{j=1}^{M}\sum_{k=1}^{K} a_{ijk}\big[x(1-x)\big]^i\big[y(1-y)\big]^{j+1}\big[z(1-z)\big]^{k+1} \tag{32}$$

$$T = \sum_{i=1}^{N}\sum_{j=1}^{M}\sum_{k=1}^{K} b_{ijk}\left[(2x-1)^{2(i-1)} - \frac{i-1}{i}(2x-1)^{2i}\right]\left[(2y-1)^{2j-1} - \frac{2j-1}{2j+1}(2y-1)^{2j+1}\right] \times \big[z(1-z)(1-2z)^{2(k-1)}\big] \tag{33}$$

Let us first solve the problem for a cubical box $A = B = 1$, and next for a box of square cross section $A = B$ but of increasing height $A = B < 1$ (we exclude $B > 1$, since the approximation (32) allows the study of a one roll system only). For the cubical box we find

$$\begin{array}{lll} N = M = K = 1 & Ra^{\text{crit}} = 3988.12 & \\ N = M = K = 2 & Ra^{\text{crit}} = 3412.91 & \Delta = 14\% \\ N = M = K = 3 & Ra^{\text{crit}} = 3406.45 & \Delta = 0.2\% \\ N = M = K = 4 & Ra^{\text{crit}} = 3406.28 & \Delta = 0.005\% \end{array}$$

The approximation $N = M = K = 4$ implies computing a 128×128 determinant for many Rayleigh numbers in order to catch its zero value (more precisely the change of sign of the determinant) and this is time consuming. In view of the result there is no need to go to a higher approximation. Even between the order $N = M = K = 2$ and the order $N = M = K = 3$ there is only a 0.2% difference. Therefore in Table 2 we limit ourselves to the approximation $N = M = K = 3$. We also compare the results of the full 3-D problem with those from the 2-D approximation that ignores the boundary conditions at the bottom and at the top of the cavity. These 2-D values are taken from Table 1 at the same approximation $N = M = 3$.

The value of 3406.28 for Ra^{crit} in a cubical box is compatible with numerical calculations of the Nusselt number Nu [36] for several types of rolls: convection (or $Nu > 1$) is found at 3500 for a single roll structure. In a box of square cross section, a diagonally oriented roll, or toroïdal shape perturbations, could lead to other critical Rayleigh numbers. In these two last cases the three velocity components are nonzero, a situation we do not account for since we are mainly interested in geometries of Fig. 1. Bergeon [37] reported for the cubical box the value $Ra^{\text{crit}} = 3388.39$. We also give in the last part of Table 2 the critical Rayleigh number for a box of rectangular cross section $P = 10L$, a situation that certainly rules out toroïdal perturbations with fluid rising at the centre and sinking near the four boundaries.

The conclusion of this table is that the lower and upper boundary conditions have no measurable effect as soon as the height becomes larger than 10 times the greatest horizontal dimension, since it is hard to measure a Rayleigh number with accuracy better than 2%.

Let us come back to the experimental cell we used in the thermogravitational problem ($H = 530$ mm; $L = 1.58$ mm; $P = 30$ mm) and look more closely at the convergence of the 3-D problem (Table 3). The first part of Table 3 shows the decrease and the convergence of Ra^{crit} when the number of trial functions in the y and z directions is increased. In the second part of the table we keep $M = K = 3$ and we increase the number of trial functions in the x direction: already with $N = 1$ four significant digits are obtained; $N = 2$ changes only the two last digits whereas with $N = 3$ the result does not change at all (six significant digits unchanged). This is essentially due to the small value of L (1.58 mm) compared to the two other dimensions ($P = 30$ mm and $H = 530$ mm). It is sufficient to take a parabolic variation for the velocity field in the x direction, and a constant for the temperature field which satisfies

Table 2
Variation of the critical Rayleigh number with the two aspect ratios ($N = M = K = 3$)

Tableau 2
Variation du nombre de Rayleigh critique en fonction des deux rapports d'aspect ($N = M = K = 3$)

Aspect ratio	Ra^{crit} for the 3-D problem	Ra^{crit} for the 2-D problem: $707.993547/B^4$	Difference between 2-D and 3-D
$A = B = 1$	0.340645×10^4	0.707994×10^3	>100%
$A = B = 1/2$	0.170906×10^5	0.113279×10^5	51%
$A = B = 1/3$	0.686800×10^5	0.573475×10^5	20%
$A = B = 1/5$	0.471615×10^6	0.442496×10^6	7%
$A = B = 1/10$	0.719247×10^7	0.707994×10^7	<2% (1.6%)
$A = B = 1/100$	0.708111×10^{11}	0.707994×10^{11}	<0.02%
$A = B = 1/1000$	0.707994×10^{15}	0.707993×10^{15}	0%
$P = 10L$; $A = B/10$	Ra^{crit} for the 3-D problem	Ra^{crit} for the 2-D problem: $13666.5038/B^4$	Difference between 2-D and 3-D
$B = 1$ $A = 1/10$	0.551436×10^5	0.136665×10^5	>100%
$B = 1/2$ $A = 1/20$	0.338969×10^6	0.218664×10^6	55%
$B = 1/3$ $A = 1/30$	0.135993×10^7	0.110699×10^7	23%
$B = 1/5$ $A = 1/50$	0.922171×10^7	0.854156×10^7	8%
$B = 1/10$ $A = 1/100$	0.139382×10^9	0.136665×10^9	2%
$B = 1/100$ $A = 1/1000$	0.136693×10^{13}	0.136665×10^{13}	0.02%
$B = 1/1000$ $A = 1/10000$	0.136665×10^{17}	0.136665×10^{17}	0%

Table 3
Convergence of the critical Rayleigh number for the experimental column

Tableau 3
Convergence du nombre de Rayleigh critique pour la colonne expérimentale

Order of approximation			$B = 30/530$; $A = 1.58/530$
N	M	K	Ra^{crit}
1	1	1	0.553753×10^{10}
1	2	2	0.470956×10^{10}
1	3	3	0.455684×10^{10}
2	3	3	0.455612×10^{10}
3	3	3	0.455612×10^{10}
1	4	4	0.450897×10^{10}
1	5	5	0.449527×10^{10}
1	6	6	0.449201×10^{10}
1	7	7	0.449133×10^{10}
1	8	8	0.449119×10^{10}

the zero heat flux condition. This is the so-called Hele-Shaw approximation used when avoiding the solution of the full equations and that is in some sense fully justified here by increasing the number of trial functions in x. However if we still increase M and K (last part of Table 3) then the significant digits still change. Four digits are correct at the order $M = K = 8$, which implies once again the computation of 128×128 determinants. Without the vertical confinement we found (2-D model) $Ra^{\text{crit}} = 0.446183 \times 10^{10}$; vertical confinement increases a little bit this number to $Ra^{\text{crit}} = 0.449119 \times 10^{10}$ as it should be. In conclusion, operating with the thermogravitational column described before, does not allow one to maintain an adverse density stratification with heavy liquid at the top, cold or 'salty' via the Soret effect according to Eq. (5).

3. The Rayleigh–Benard problem in confined cavities for binary fluids

We now investigate the same problem as exposed in the previous paragraph, but the cavity is filled with a binary mixture. Due to the Soret effect a steady concentration gradient (or better, mass fraction gradient) $\mathrm{d}C^{\text{st}}/\mathrm{d}z$ will be established, proportional to the temperature gradient.

$$\frac{\mathrm{d}C^{\mathrm{st}}}{\mathrm{d}z} = -\frac{D_T}{D} C_0(1-C_0)\frac{\mathrm{d}T^{\mathrm{st}}}{\mathrm{d}z} \tag{34}$$

where D_T is the thermodiffusion coefficient and D the isothermal diffusion coefficient. We are only interested here in the particular case $D_T/D > 0$. In other words, $\mathrm{d}C^{\mathrm{st}}/\mathrm{d}z$ has the opposite sign of $\mathrm{d}T/\mathrm{d}z$. Since $\mathrm{d}T/\mathrm{d}z < 0$ (we heat from below), $\mathrm{d}C^{\mathrm{st}}/\mathrm{d}z > 0$ and the considered component goes to the top, thus to the cold wall. We have now to specify which component we are speaking on. We take arbitrarily the denser component, but the opposite choice could equally be made. Indeed we need an equation of state

$$\rho = \rho_0\big[1-\alpha(T-T_0)+\beta(C-C_0)\big] \tag{35}$$

and β, the mass expansion coefficient given by $\frac{1}{\rho_0}\frac{\partial\rho}{\partial C}$ is thus positively defined. Had we taken the lighter component as the reference component, then β would be negative. But the important parameter is the solutal contribution to the buoyancy force, compared to the thermal contribution, that we call S; combining Eqs. (34), (35) S is equal to (see also Eq. (4))

$$S = \frac{\beta\frac{\mathrm{d}C^{\mathrm{st}}}{\mathrm{d}z}}{-\alpha\frac{\mathrm{d}T^{\mathrm{st}}}{\mathrm{d}z}} = +\frac{\beta}{\alpha}\frac{D_T}{D}C_0(1-C_0) \tag{36}$$

Therefore a different choice for the reference component would leave unchanged the sign of S, since both β and D_T would change sign. Thus to be more concrete, we are interested in the case $S > 0$, that is to say the temperature and the concentration gradients are cooperating; since the temperature gradient is destabilizing, so is the concentration gradient: the denser component goes to the cold upper plate.

The linear stability of the laterally unbounded liquid layer with upper and lower stress free boundaries and permeable to matter, leads to Eq. (6a) for the critical Rayleigh number (or to Eq. (6b) for rigid boundaries) and as explained in details in the introduction this cannot be used to determine the separation ratio based on the onset of convection. We want to generalise the results presented in Section 2 in order to see if we can use these results as a possible new way of measurement of the Soret coefficient by a noninvasive technique (i.e. the detection of the onset of convection by e.g. LDV or PIV).

Without going into the details of the adimensionalisation process, except that the field C is scaled by $(D_T/D)C_0(1-C_0)\Delta T$, let us rewrite Eq. (17) for the binary mixture

$$\nabla^2\left(\frac{\partial^2\psi}{\partial z^2}+\frac{1}{B^2}\frac{\partial^2\psi}{\partial y^2}\right) = \frac{Ra}{B}\left(\frac{\partial T}{\partial y}-S\frac{\partial C}{\partial y}\right) \tag{37}$$

The second term in the r.h.s. arises from the solutal contribution to the buoyancy and the minus sign from the choice we made for the equation of state (35). The heat equation (18) is unchanged (rewritten here for simplicity)

$$\frac{1}{B}\frac{\partial\psi}{\partial y} = \nabla^2 T \tag{18}$$

but we need an additional equation for the conservation of mass of the heavy component

$$-\frac{1}{B}\frac{\partial\psi}{\partial y} = \frac{1}{Le}\big(\nabla^2 C+\nabla^2 T\big) \tag{38}$$

This equation is similar to that for the energy, but there are two differences; the minus sign in the l.h.s. is due to the fact that the steady gradients $\Delta T/H$ and $\Delta C/H$ are of opposite sign according to Eq. (34); in the r.h.s. of (38), in the divergence of the mass flux, there is a term describing the Soret effect. Le is the Lewis number already mentioned in the introduction. The boundary conditions for ψ and T are of course the same as before. We need boundary conditions for C: physically, the mass flux $\vec{J}$ across a solid boundary is zero, i.e. in a dimensional form.

$$-\rho_0 D\,\mathrm{grad}\,C-\rho_0 D_T C_0(1-C_0)\,\mathrm{grad}\,T = 0 \quad \text{across a boundary} \tag{39a}$$

or in a nondimensional form

$$\mathrm{grad}\,C+\mathrm{grad}\,T = 0 \tag{39b}$$

If a boundary is adiabatic (e.g. the four lateral boundaries), then the boundary conditions on T and C are the same. On the contrary, if a boundary is at prescribed temperature (the lower and the upper), than the full condition (39a) or (39b) applies.

Before solving the full 3-D problem, let us once again have a look at the 2-D problem for which the different fields ψ, T and C do not depend on the vertical coordinate z. Then Eqs. (37), (18), (38) reduce to

$$\nabla^2_{x,y} V_z = -Ra(T - SC) \tag{40}$$

$$(-V_z) = \nabla^2_{x,y} T \tag{18}$$

$$\nabla^2_{x,y} T + \nabla^2_{x,y} C = Le\, V_z \tag{41}$$

There is thus one velocity component function of the two space coordinates x and y. It is rather easy to eliminate the variables T and C in the system (40), (41) and to obtain a fourth order equation similar to Eq. (23)

$$\nabla^4_{x,y} V_z = Ra\big[1 + S(Le + 1)\big] V_z \tag{42}$$

which is formally the same equation as in a pure fluid provided that the Rayleigh number is multiplied by $[1 + S(Le + 1)]$. The numerical values of $Ra[1 + S(Le + 1)]$ will be those given in Table 1, provided that V_z obeys for the binary mixture case the same boundary condition as in the pure component case. But this is actually true because the boundary conditions for T and C are the same on the four lateral boundaries. In particular the *two* conditions $\partial T/\partial x = 0$ and $\partial C/\partial x = 0$ imply only from Eq. (40) *one* additional condition for V_z, namely $\nabla^2_{x,y}(\partial V_z/\partial x) = 0$ the same as for a pure fluid; the same holds for the other pair of faces. The conclusion is that when the bottom and top boundary conditions may be ignored, the critical Rayleigh number for the binary mixture is given by Eq. (7) where Ra_0^{crit} are given by the values of Table 1. Of course this conclusion is no longer true when the boundary conditions at $Z = 0$ and $Z = 1$ are taken into account.

For the full 3-D problem, one could still eliminate T and C between Eqs. (37), (18) and (38) and get a 6th order differential equation for ψ, identical in the pure component and in the binary fluid case, but the boundary conditions on ψ would be different in the two cases since at the horizontal boundaries one has $T = 0$ and $\partial C/\partial z + \partial T/\partial z = 0$; and the boundary conditions on the eliminated variables must be equivalent to the new boundary conditions on the remaining variable. Thus even if the variable ψ obeys the same differential equation, the boundary conditions would be different in the one component and in the two component cases, leading to different eigenvalues or critical Rayleigh numbers.

In view of the boundary condition (39b), it is quite natural to define a new field ζ by

$$\zeta = C + T \tag{43}$$

and the problem (37), (18) and (38) is transformed into

$$\nabla^2\left(\frac{\partial^2\psi}{\partial z^2} + \frac{1}{B^2}\frac{\partial^2\psi}{\partial y^2}\right) = \frac{Ra}{B}\left((1 + S)\frac{\partial T}{\partial y} - S\frac{\partial \zeta}{\partial y}\right) \tag{44}$$

$$\frac{1}{B}\frac{\partial\psi}{\partial y} = \nabla^2 T \tag{18}$$

$$-\frac{1}{B}\frac{\partial\psi}{\partial y} = \frac{1}{Le}\big(\nabla^2\zeta\big) \tag{45}$$

and the boundary conditions for ζ become

$$\begin{aligned} &\text{at } y = 0 \text{ and } 1 \quad \tfrac{\partial\zeta}{\partial y} = 0 \\ &\text{at } x = 0 \text{ and } 1 \quad \tfrac{\partial\zeta}{\partial x} = 0 \\ &\text{at } z = 0 \text{ and } 1 \quad \tfrac{\partial\zeta}{\partial z} = 0 \end{aligned} \tag{46}$$

The symmetry requirements for the field ζ are the same as for T. And since the boundary conditions on the four lateral boundaries are also the same for T and ζ, quite naturally we take the same expansion in X and in Y. The Z dependence of the field ζ should be different from that of T since the boundary conditions are different at $Z = 0$ and 1. Since ζ is even in Z (as it was in X) and obeys at $Z = 0$ and 1 the same conditions as in $X = 0$ and 1, we take the same dependence in Z and in X.

Table 4
Convergence of the critical Rayleigh number $Le = 100$

Tableau 4
Convergence du nombre de Rayleigh critique $Le = 100$

	$A = B = 1$			Eq. (7)
	$N = M = K = 1$	$N = M = K = 2$	$N = M = K = 3$	
$S = 0$	3988.122	3412.910	3406.447	
$S = 0.1$	253.941	209.095	208.902	306.887
$S = 0.2$	131.146	107.835	107.739	160.681
$S = 0.3$	88.399	72.652	72.588	108.832
$S = 0.4$	66.669	54.779	54.731	82.281
$S = 0.5$	53.514	43.963	43.925	66.145

$$\zeta = \sum_{i=1}^{N}\sum_{j=1}^{M}\sum_{k=1}^{K} c_{ijk}\left[(2x-1)^{2(i-1)} - \frac{i-1}{i}(2x-1)^{2i}\right]\left[(2y-1)^{2j-1} - \frac{2j-1}{2j+1}(2y-1)^{2j+1}\right] \times \left[(2z-1)^{2(k-1)} - \frac{k-1}{k}(2z-1)^{2k}\right] \tag{47}$$

This terminates the 3-D formulation of the stability of the Rayleigh Benard problem with Soret effect in very confined geometries where x-rolls prevail. An example of convergence is given in Table 4. In Table 5, we give the critical Rayleigh number, called "3-D" using the expansion (47) with $N = M = K = 3$ and we compare with Eq. (7) where $Ra_0^{\text{crit}}(\frac{H}{L}, \frac{H}{P})$ is found by putting $S = 0$ at the same level of approximation. Clearly when $A = B \geqslant 1/10$, the approximation (7) cannot be used because of the importance of the difference between top and bottom boundary conditions on the concentration field (or the ζ field) and on the temperature field. On the other hand, when $A = B < 1/10$, the correct top and bottom boundary conditions on the concentration field can be ignored since these boundaries are far away and the approximation (7) can be used. The values listed in Table 5 has been computed for a cavity of square cross section $A = B$, but, as a matter of fact, the program runs for any value of $A \neq B$, with the same physical interpretation: as soon as the height of the cell becomes greater than 10 times the largest horizontal dimension, the exact top and bottom boundary conditions for the concentration (or ζ) field loose their importance.

We now search for a possible 'design' for a new observation cell. The first limitation is the relaxation time for the diffusion process $\tau_{\text{Diff}} = H^2/(\pi^2 D)$. Based on the approximate order of magnitude $D \sim 10^{-9}$ m^2/s, the requirement $\tau_{\text{Diff}} < 24$ hours limits the height of the column at $H = 3$ cm. That means that after each temperature change, we have to wait 5 times the relaxation time (5 days) before the new steady state is reached and the next temperature change. Experiments with diffusion processes always require some patience, but 5 days is not too bad owing to the fact that in packed thermogravitational column the steady state is achieved typically after 90 days, see e.g. [38]. Putting the thermophysical properties of pure water in the definition of the Rayleigh number together with $H = 0.03$ m, we find $Ra \sim 3.645 \times 10^5 \Delta T$. A second limitation is on ΔT for the Boussinesq approximation to be valid, say $\Delta T < 30\,^{\circ}$C ($\alpha \Delta T \sim 0.01 \ll 1$). Therefore the critical Rayleigh number should be of the order of 10^7. Looking at Table 2, $B = 1/5$ and $A = 1/50$ should be perfect. But $A = 1/50$ implies for $H = 30$ mm the value $L = 0.6$ mm, which is not very comfortable for an accurate construction of the cell, and moreover the cell will be difficult to fill for capillarity reasons. Therefore we looked at a different shape: $H = 30$ mm; $L = 2$ mm and $P = 3$ mm ($A = 1/15$ and $B = 1/10$). Table 6 gives for these dimensions ($A = 1/15$ and $B = 1/10$) the critical Rayleigh number and the corresponding critical ΔT for the properties of pure water, even if for $S \neq 0$ these properties (density, viscosity, ...) will change a little bit, but not so much if you have in mind dilute sodium chloride or copper sulphate solutions. What Table 6 shows, is that experiments seem possible with the drop of the critical ΔT from 25 °C to ∼1 °C. However, since we are in the Soret regime, the velocity amplitudes remain small and this raises the question of the detection of small velocities. An observation cell has been built with dimensions given above and is now under evaluation tests for pure water using Particle Image Velocimetry PIV. Even if the first experimental result is promising, at this stage more details will be outside the scope of this paper.

Table 5
Critical Rayleigh number function of the cross section aspect ratio and separation ratio, $Le = 100$, $N = M = K = 3$

Tableau 5
Nombre de Rayleigh critique en fonction du rapport d'aspect transversal et du rapport de séparation, $Le = 100$, $N = M = K = 3$

$A = B =$	1		1/2		1/3	
	"3-D"	Eq. (7)	"3-D"	Eq. (7)	"3-D"	Eq. (7)
$S = 0.0$	3406.447	3406.447	17090.589	17090.589	68680.016	68680.016
$S = 0.1$	208.902	306.887	1424.614	1539.693	6030.060	6187.389
$S = 0.2$	107.739	160.681	743.182	806.160	3153.170	3239.623
$S = 0.3$	72.588	108.832	502.716	546.025	2134.711	2194.250
$S = 0.4$	54.731	82.281	379.820	412.816	1613.544	1658.938
$S = 0.5$	43.925	66.145	305.145	331.856	1296.915	1333.593

$A = B =$	1/5		1/10		1/50	
	"3-D"	Eq. (7)	"3-D"	Eq. (7)	"3-D"	Eq. (7)
$S = 0$	471614.97	471614.97	0.719347×10^7	0.719347×10^7	0.442788×10^{10}	0.442788×10^{10}
$S = 0.1$	42258.34	42487.84	0.647888×10^6	0.648060×10^6	0.398903×10^9	0.398908×10^9
$S = 0.2$	22119.66	22245.99	0.339220×10^6	0.339315×10^6	0.208859×10^9	0.208862×10^9
$S = 0.3$	14980.51	15067.57	0.229758×10^6	0.229823×10^6	0.141464×10^9	0.141466×10^9
$S = 0.4$	11325.27	11391.67	0.173705×10^6	0.173755×10^6	0.106952×10^9	0.106954×10^9
$S = 0.5$	9103.91	9157.57	0.139639×10^6	0.139679×10^6	0.085977×10^9	0.085978×10^9

$A = B =$	1/100		1/250		1/1000	
	"3-D"	Eq. (7)	"3-D"	Eq. (7)	"3-D"	Eq. (7)
$S = 0$	0.708111×10^{11}	0.708111×10^{11}	0.276567×10^{13}	0.276567×10^{13}	0.707995×10^{15}	0.707995×10^{15}
$S = 0.1$	0.637928×10^{10}	0.637938×10^{10}	0.249156×10^{12}	0.249159×10^{12}	0.637823×10^{14}	0.637833×10^{14}
$S = 0.2$	0.334009×10^{10}	0.334015×10^{10}	0.130454×10^{12}	0.130456×10^{12}	0.333954×10^{14}	0.333960×10^{14}
$S = 0.3$	0.226230×10^{10}	0.226234×10^{10}	0.088359×10^{12}	0.088360×10^{12}	0.226193×10^{14}	0.226196×10^{14}
$S = 0.4$	0.171038×10^{10}	0.171041×10^{10}	0.066803×10^{12}	0.066804×10^{12}	0.171010×10^{14}	0.171013×10^{14}
$S = 0.5$	0.137495×10^{10}	0.137497×10^{10}	0.053702×10^{12}	0.053702×10^{12}	0.137472×10^{14}	0.137475×10^{14}

Table 6
Possible experiments with $H = 30$ mm, $L = 2$ mm and $P = 3$ mm, $Le = 100$; $N = M = K = 3$

Tableau 6
Expérience possible avec $H = 30$ mm, $L = 2$ mm et $P = 3$ mm, $Le = 100$; $N = M = K = 3$

$B = 1/10$; $A = 1/15$	Ra^{crit} for the 3-D problem	ΔT^{crit} (with the physical properties of water)
$S = 0$	0.916770×10^7	25.2 °C
$S = 0.1$	0.825708×10^6	2.3 °C
$S = 0.2$	0.432322×10^6	1.2 °C
$S = 0.3$	0.292818×10^6	0.8 °C
$S = 0.4$	0.221381×10^6	0.6 °C
$S = 0.5$	0.177964×10^6	0.5 °C

4. Conclusions

In this article we have calculated the critical Rayleigh number for a laterally extremely confined quiescent liquid layer submitted to an adverse vertical density gradient, with and without the Soret effect. These calculations were always conducted keeping in mind experimental evidence, existing or forthcoming.

In the existing thermogravitational column ($H = 530$ mm; $P = 30$ mm; $L = 1.58$ mm) we have shown that the (solutal) Rayleigh number at which the column operates with salt on top (or water in water–alcohol systems), was supercritical and this could explain the absence of any separation. Of course we did not incorporate the basic velocity profile, which is a much more complicated problem left for future investigation. Also to be complete, the calculations should be repeated in cylindrical coordinates in order to see the differences with parallelepipedic columns, if any.

Incorporating the Soret effect, we have shown that the decrease of the critical Rayleigh number for positive separation ratios was of the same order as for horizontally extended systems. However, confining laterally the system increases the value of the critical point and the deduced critical temperature difference seems to be accessible to experimental investigation. Thus this finding could lead to a new way of determination of positive separation ratios by convective coupling. However, as shown by Eq. (45), the theory requires the knowledge of the Lewis number, in other words of the diffusion coefficient D. Convective coupling will give the separation ratio proportional to D_T/D. Thus the proposed method will allow the determination of D_T that could be compared to the value coming from thermogravitational column according to Eq. (1) based on a sampling process along the column height. In contradistinction, what we propose here does not imply any sampling and chemical analysis of removed samples. Should the two values agree, then we could have confidence in the proposed value for D_T.

References

[1] S. Chandrasekhar, Hydrodynamic and Hydromagnetic Stability, Oxford University Press, Clarendon, 1961, pp. 9–75.
[2] J.K. Platten, J.-Cl. Legros, Convection in Liquids, Springer, Berlin, 1984 (Chapter IX).
[3] J.K. Platten, A variational formulation for the stability of flows with temperature gradients, Int. J. Engrg. Sci. 9 (1971) 855–869.
[4] J.-Cl. Legros, J.K. Platten, The two component Bénard problem with Poiseuille flow, J. Non-Equilib. Thermodyn. 2 (4) (1977) 211–232.
[5] Ch. Jung, M. Lücke, P. Büchel, Influence of through-flow on linear pattern formation properties in binary mixture convection, Phys. Rev. E 54 (1996) 1510–1529.
[6] E. Piquer, M.C. Charrier-Mojtabi, M. Azaiez, A. Mojtabi, Convection mixte en fluide binaire avec effet Soret : étude analytique de la transition vers les rouleaux 2d, C. R. Mecanique 333 (2005) 179–186.
[7] S.H. Davis, Convection in a box: linear theory, J. Fluid Mech. 30 (1967) 465–478.
[8] O. Ecenarro, J.A. Madariaga, J. Navarro, C.M. Santamaria, J.A. Carrion, J.M. Saviron, Thermogravitational thermal diffusion in liquid polymer solutions, Macromolecules 27 (1994) 4968–4971.
[9] M.M. Bou-Ali, O. Ecenarro, J.A. Madariaga, C.M. Santamaria, J.J. Valencia, Thermogravitational measurement of the Soret coefficient of liquid mixtures, J. Phys.: Condens. Matter 10 (1998) 3321–3331.
[10] M.M. Bou-Ali, O. Ecenarro, J.A. Madariaga, C.M. Santamaria, J.J. Valencia, Soret coefficient of some binary liquid mixtures, J. Non-Equilib. Thermodyn. 24 (1999) 228–233.
[11] J.K. Platten, M.M. Bou-Ali, J.-F. Dutrieux, Precise determination of the Soret, thermodiffusion and isothermal diffusion coefficients of binary mixtures of dodecane, isobutylbenzene and 1,2,3,4-tetrahydronaphtalene, Philosophical Magazine 83 (17–18) (2003) 2001–2010.
[12] M.M. Bou-Ali, J.J. Valencia, J.A. Madariaga, C. Santamaria, O. Ecenarro, J.-F. Dutrieux, Determination of the thermodiffusion coefficient in three binary organic liquid mixtures by the thermogravitational method, Philosophical Magazine 83 (17–18) (2003) 2011–2015.
[13] J.-F. Dutrieux, Contributions à la métrologie du coefficient Soret, Ph.D. thesis, University of Mons-Hainaut, Belgium, 2002.
[14] M.M. Bou-Ali, J.K. Platten, J.A. Madariaga, C.M. Santamaria, Soret effect convective coupling and instabilities in thermogravitational column, in: J.P. Meyer, A.G. Malan (Eds.), Proceedings of the 4th International Conference on Heat Transfer, Fluid Mechanics and Thermodynamics HEFAT 2005, Cairo, Egypt, 19–22 September 2005, paper BM1.
[15] M.M. Bou Ali, O. Ecenarro, J.A. Madariaga, C.M. Santamaria, Stability of convection in a vertical binary fluid layer with an adverse density gradient, Phys. Rev. E 59 (1) (1999) 1250–1252.
[16] W.H. Furry, R.C. Jones, L. Onsager, On the theory of isotope separation by thermal diffusion, Phys. Rev. 55 (1939) 1083–1095.
[17] S.D. Majumdar, The theory of separation of isotopes by thermal diffusion, Phys. Rev. 81 (1951) 844–848.
[18] G. Labrosse, Boussinesq approximation, and beyond, in tall thermo-gravitational column, C. R. Mecanique 335 (2007), this issue; DOI: 10.1016/j.crme.2007.08.012.
[19] G. Chavepeyer, J.K. Platten, Simulation numérique 2D de la séparation dans une colonne de thermogravitation et comparaison avec la théorie de Furry–Jones–Onsager–Majumdar, Entropie 198/199 (1996) 25–29.
[20] S.J. Linz, M. Lücke, Convection in binary mixtures: A Galerkin model with impermeable boundary conditions, Phys. Rev. A 35 (1987) 3997–4000.
[21] J.K. Platten, J.-F. Dutrieux, G. Chavepeyer, Soret effect and free convection: a way to measure Soret coefficients, in: W. Köhler, S. Wiegand (Eds.), Thermal Nonequilibrium Phenomena in Fluid Mixtures, in: Lecture Notes in Physics, vol. 584, 2002, pp. 313–333.
[22] O. Lhost, J.K. Platten, Transition between steady states, traveling waves and modulated waves in the system water–isopropanol heated from below, Phys. Rev. A 38 (6) (1988) 3147–3150.
[23] H. Touiri, J.K. Platten, G. Chavepeyer, Effect of the separation ratio on the transition between travelling waves and steady convection in the two-component Rayleigh–Benard problem, Eur. J. Mech., B/Fluids 15 (2) (1996) 241–257.
[24] R.J. Schmidt, S.W. Milverton, On the instability of a fluid when heated from below, Proc. Roy. Soc. A 152 (1935) 586–594.
[25] J.K. Platten, G. Chavepeyer, Oscillatory motion in Bénard cell due to the Soret effect, J. Fluid Mech. 60 (1973) 305–319.
[26] J.K. Platten, D. Villers, O. Lhost, LDV study of some free convection problems at extremely slow velocities: Soret driven convection and Marangoni convection, in: R.J. Adrian, T. Asanuma, D.F.G. Durão, F. Durst, J.H. Whitelaw (Eds.), Laser Anemometry in Fluid Mechanics, vol. 3, LADOAN—Instituto Superior Técnico, Lisbon, 1988, pp. 245–260.
[27] O. Lhost, Contribution expérimentale à l'étude de la convection libre induite par effet Soret, Ph.D. thesis, University of Mons, 1990.
[28] P. Kolodner, H. Williams, C. Moe, Optical measurement of the Soret coefficient of ethanol/water solutions, J. Chem. Phys. 88 (10) (1988) 6512–6524.

[29] K.J. Zhang, M.E. Briggs, R.W. Gammond, J.V. Sengers, Optical measurement of the Soret coefficient and the diffusion coefficient of liquid mixtures, J. Chem. Phys. 104 (1996) 6881–6892.
[30] S. Wiegand, W. Köhler, Measurement of transport coefficients by an optical grating technique, in: W. Köhler, S. Wiegand (Eds.), Thermal Nonequilibrium Phenomena in Fluid Mixtures, in: Lecture Notes in Physics, vol. 584, 2002, pp. 189–210.
[31] M.G. Velarde, R.S. Schechter, Thermal diffusion and convective stability: an analysis of the convected fluxes, Phys. Fluids 15 (1972) 1707–1714.
[32] A. Mojtabi, J.K. Platten, M.-C. Charrier-Mojtabi, Onset of free convection in solutions with variable Soret coefficients, J. Non-Equilib. Thermodyn. 27 (2002) 25–44.
[33] J. Boussinesq, Théorie analytique de la chaleur, Gauthiers-Villars, Paris, 1903.
[34] C.-S. Yih, Thermal instability of a viscous fluid, Quart. Appl. Math. 17 (1959) 25–42.
[35] R.A. Wooding, Instability of a viscous liquid of variable density in a vertical Hele-Shaw cell, J. Fluid Mech. 7 (1960) 501–515.
[36] J. Pallares, F.X. Grau, F. Giralt, Flow transitions in laminar Rayleigh–Benard convection in a cubical cavity at moderate Rayleigh numbers, Int. J. Heat Mass Trans. 42 (1999) 753–769.
[37] A. Bergeon, University Paul Sabatier and Institut de Mécanique des Fluides, Toulouse, private communication.
[38] P. Costesèque, D. Fargue, P. Jamet, Thermodiffusion in porous media and its consequences, in: W. Köhler, S. Wiegand (Eds.), Thermal Nonequilibrium Phenomena in Fluid Mixtures, in: Lecture Notes in Physics, vol. 584, 2002, pp. 389–427.